Chapter 5

Surface Ribbon Technique

Earlier in this century with increased usage of electricity, inductance calculations found applications in power distribution networks. Grover [12] gave an extensive treatment on inductance and introduced the filament technique. More recently, as the frequency of interest increased in integrated circuitry, inductance of interconnects has become more important in estimating delay and cross-talk. In 1972, Ruehli [31] introduced the partial inductance concept so that geometries that did not form a loop could be modeled. In 1979, Weeks [39] applied Ruehli's concepts in two dimensions and introduced a filament technique for multi-conductor transmission line structures. The advantage of Weeks' technique was that the calculation of coefficients was through an analytic function. Weeks' and Ruehli's techniques generate dense matrices to represent the interconnect structure under consideration. Later, new techniques were introduced to accelerate the filament technique solutions. Some of them worked on the physics of the problem to throw away unnecessary information (e.g., the contributions from internal parts of conductors at high frequencies [35]) and some others worked on the mathematical side to improve solution speed,

as in FastHenry[1]. In this chapter, a modified filament technique will be introduced using the Effective Internal Impedance approach (EII). With the EII, the volume of conductors are represented at their surfaces. Meshing conductors on the surface results in ribbons which are used to calculate the interaction between surface regions on the conductors. Calculation of internal behavior through an analytic function and meshing only at the surface reduces problem size and accelerates the solution process[37]. To investigate the validity, the ribbon technique results will be compared to measurement and filament technique results.

5.1 Filament Technique

In a multi-conductor transmission line the current distribution over the cross section of the conductors is a function of frequency. A step function approximation of the current distribution leads to the filament technique. Each conductor segment is divided into filaments which run the length of the conductor (Fig. 5.1.a). The current on each filament is assumed to be uniform over its cross section. The voltage drop per unit length in a filament is a function of the current flowing in the filament plus the induced voltage due to the currents on other filaments,

$$V_i = I_i R_i + \sum_{k=1}^{N} I_k j\omega L_{ik}, \tag{5.1}$$

where V_i and I_i are the voltage drop and the current through the ith filament, respectively, and N is the total number of filaments. R_i is the dc resistance of

[1] Fasthenry is an inductance and resistance calculation tool based on filament technique with a multipole-accelerated Generalized Minimal Residual (GMRES) matrix solution algorithm [22].

the filament and L_{ik}'s are the self and mutual inductances (Fig. 5.1.b). Since this is a truly two dimensional structure, the voltage drop per unit length in a conductor should be the same for all its filaments. Equation (5.1) can be written in matrix form as

$$\begin{bmatrix} R_1 + j\omega L_{11} & j\omega L_{12} & \dots & j\omega L_{1N} \\ j\omega L_{12} & R_2 + j\omega L_{22} & \dots & j\omega L_{2N} \\ \vdots & \vdots & \ddots & \vdots \\ j\omega L_{1N} & j\omega L_{2N} & \dots & R_N + j\omega L_{NN} \end{bmatrix} \begin{bmatrix} I_1 \\ I_2 \\ \vdots \\ I_N \end{bmatrix} = \begin{bmatrix} V_1 \\ V_2 \\ \vdots \\ V_N \end{bmatrix}. \quad (5.2)$$

The dense impedance matrix in (5.2) is inverted to solve for the unknown current. By summing the currents that flow through the filaments that belong to a conductor, the inverted impedance matrix for the filaments can be reduced to the admittance matrix for the conductors. Thus,

$$\mathbf{I} = \mathbf{y}\mathbf{V}, \quad (5.3)$$

where $\mathbf{I}$ is the vector representing the currents on conductors and $\mathbf{y}$ is the admittance matrix of conductors. The entries of $\mathbf{y}$ are calculated using

$$y_{pq} = \sum_{l,m} Y_{lm}, \quad (5.4)$$

where Y_{lm}'s are the entries in the inverse of the impedance matrix in (5.2), and filament "l" is in conductor "p" and filament "m" is in conductor "q". The total frequency dependent series impedance matrix for a multi-conductor transmission line is calculated by inverting the $\mathbf{y}$ matrix.

The electromagnetics side of the problem is to calculate the entries of the matrix in (5.2). The resistive terms which appear on the diagonal (denoted by R_i) are the dc resistance of each filament calculated as

$$R_i = \frac{\ell}{\sigma_i w_i h_i}, \quad (5.5)$$

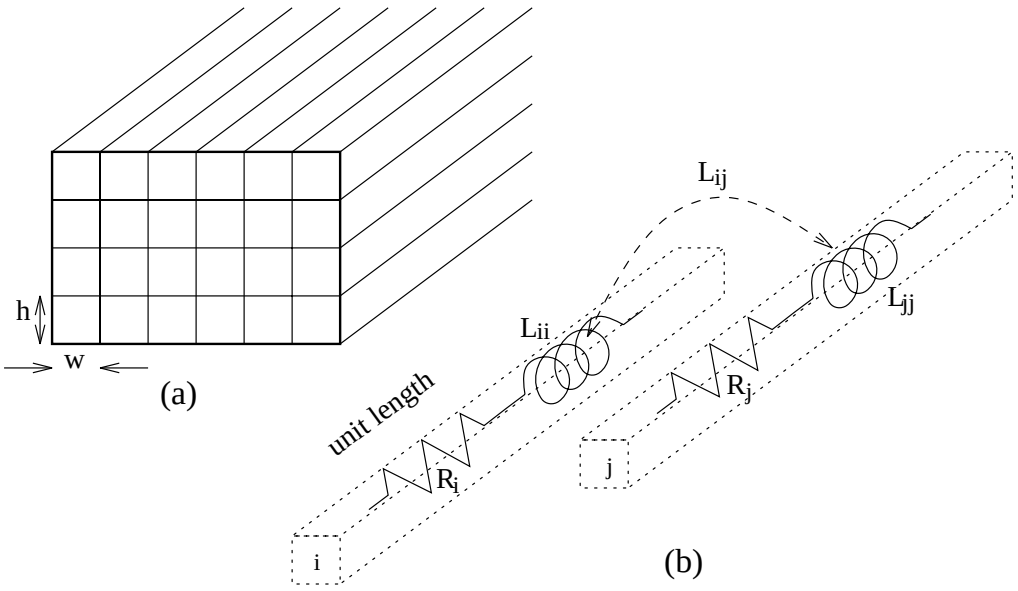

Figure 5.1: Weeks' filament technique: (a) Each conductor is subdivided into filaments, 'w' wide and 'h' thick. (b) Voltage drop per unit length on ith filament as a function of resistance R_i, self inductance L_{ii} and sum of all mutuals $\sum_j L_{ij}$.

where ℓ, w_i, and h_i are the length, width, and height of the filament, respectively, and σ_i is the conductivity of the conductor which the filament is in.

Assuming the net current is zero in the whole structure, the self and mutual inductance terms (diagonal and off diagonal, respectively) are calculated through an integral equation,

$$L_{ij} = -\frac{\mu}{4\pi w_i w_j h_i h_j} \times \int_{x_i-\frac{w_i}{2}}^{x_i+\frac{w_i}{2}} \int_{y_i-\frac{h_i}{2}}^{y_i+\frac{h_i}{2}} \int_{x_j-\frac{w_j}{2}}^{x_j+\frac{w_j}{2}} \int_{y_j-\frac{h_j}{2}}^{y_j+\frac{h_j}{2}} \ln\left[(x-x')^2+(y-y')^2\right] dy'dx'dydx. \tag{5.6}$$

The integral in (5.6) can be evaluated in closed form [39, 35], thus the calculation of entries in the impedance matrix are accelerated.

Weeks' filament technique is very efficient at low frequencies where the

skin-effect is not dominant. As the frequency increases, several of segments are needed to capture the decaying current profile in the sample (i.e., the filament size has to be smaller than the skin-depth). An adaptive meshing scheme can be devised to generate filaments depending on the frequency and the conductivity of conductors. At each frequency point the impedance matrix for the filaments has to be calculated and inverted, which for practical cases will be time consuming. One way of overcoming this problem is to use the effective internal impedance approach explained in Chapter 3.

5.2 Surface Ribbon Technique

The massive and dense matrices generated by the filament technique to capture the proximity and skin effects as the frequency increases demand long computation time and vast computer resources. The filament technique requires the current distribution to be sampled well enough with filaments to obtain an accurate result. As the current crowds towards the surface due to skin-effect, the filament dimensions have to be scaled to accommodate the change in the current distribution. By using the effective internal impedance approach explained in Chapter 3, the problem can be changed from a volume to a surface one. An effective internal impedance shell replaces the conductor at the surface, that has the correct frequency dependence on the surface as the original conductor. Then, the surface currents on the effective internal impedance shell can be sampled using ribbons, analogous to filaments for the volume filament technique. The proximity effect is captured by the interactions between the ribbons.

On each ribbon the current density is assumed uniform, hence the surface

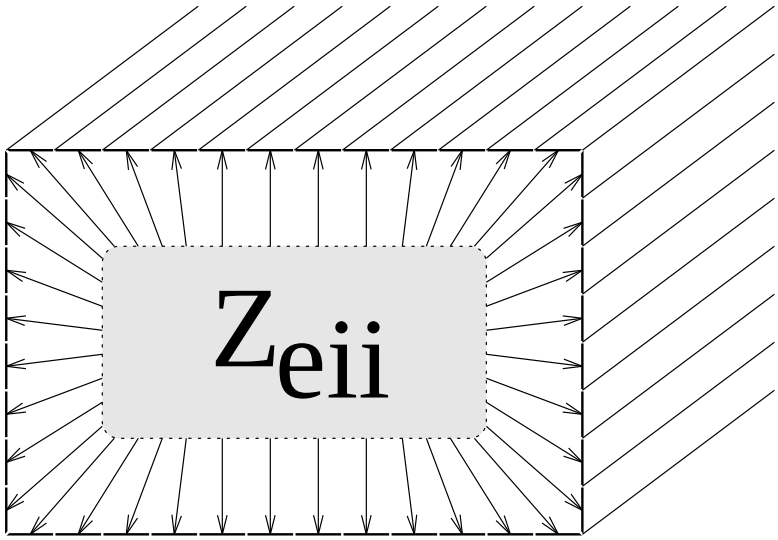

Figure 5.2: The Ribbon Technique, inside of conductor is represented on the surface by using the effective internal impedance concept.

current distribution is sampled with a step function. The interaction between the ribbons is derived from (5.6) by using rectangular conductors of zero thickness. The derivation of inductance expressions for parallel (Fig. 5.3.a) and perpendicular (Fig. 5.3.b) strips are given in Appendix B.

The physics of the problem is changed from currents flowing through the volume of conductors to currents flowing on the surface of an impedance shell. The series impedance matrix is written as the mutual interactions between ribbons on the off-diagonal and the self inductance plus the effective internal impedance of ribbons on the diagonal

$$\begin{bmatrix} Z_1^{eii}+j\omega L_{11} & j\omega L_{12} & \dots & j\omega L_{1N} \\ j\omega L_{12} & Z_2^{eii}+j\omega L_{22} & \dots & j\omega L_{2N} \\ \vdots & \vdots & \ddots & \vdots \\ j\omega L_{1N} & j\omega L_{2N} & \dots & Z_N^{eii}+j\omega L_{NN} \end{bmatrix} \begin{bmatrix} I_1 \\ I_2 \\ \vdots \\ I_N \end{bmatrix} = \begin{bmatrix} V_1 \\ V_2 \\ \vdots \\ V_N \end{bmatrix}, \tag{5.7}$$

where Z^{eii}'s are the effective internal impedances assigned to each ribbon and

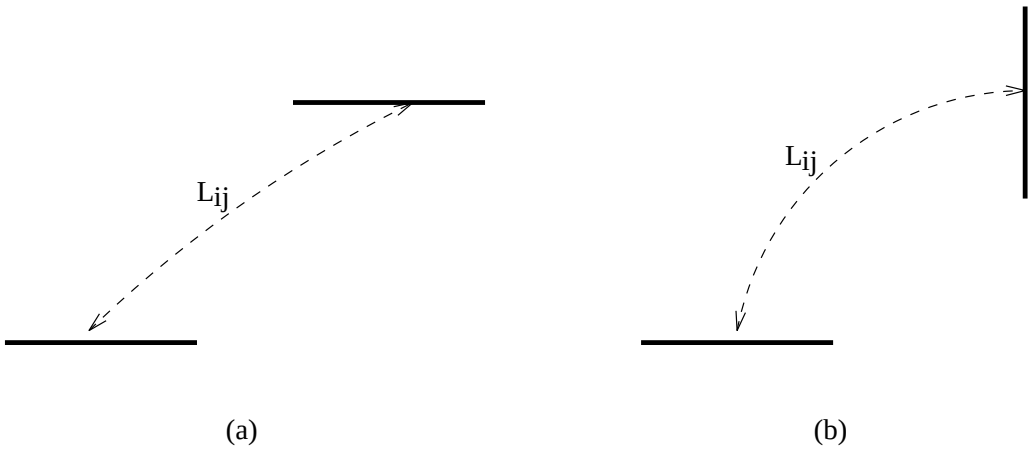

Figure 5.3: Mutual inductance cases for ribbon configurations, (a) parallel ribbons; (b) perpendicular ribbons. Current flows in a direction normal to the plane of the page.

L_{ij}'s are the self and mutual inductance terms for the ribbons. The frequency dependence is captured with the parallel summation of ribbons belonging to a conductor, just as with the filament technique (proximity effect), plus the effective internal impedance terms (skin-effect).

5.2.1 Comparison of Ribbon with Filament Technique

To calculate the frequency dependent resistance and inductance, the filament technique meshes the volume of conductors and the solution is obtained from the mutual interactions of filaments with each other. In the ribbon technique, the problem is divided into two parts, an internal and an external one. The external problem, analogous to the filament technique, solves the mutual interactions between the surface points of conductors. The internal problem is solved using the effective internal impedance approach. The filament technique captures the skin-effect as a result of mutual interactions of the filaments in a conductor. The ribbon technique readily accounts for the skin-effect through an analytical

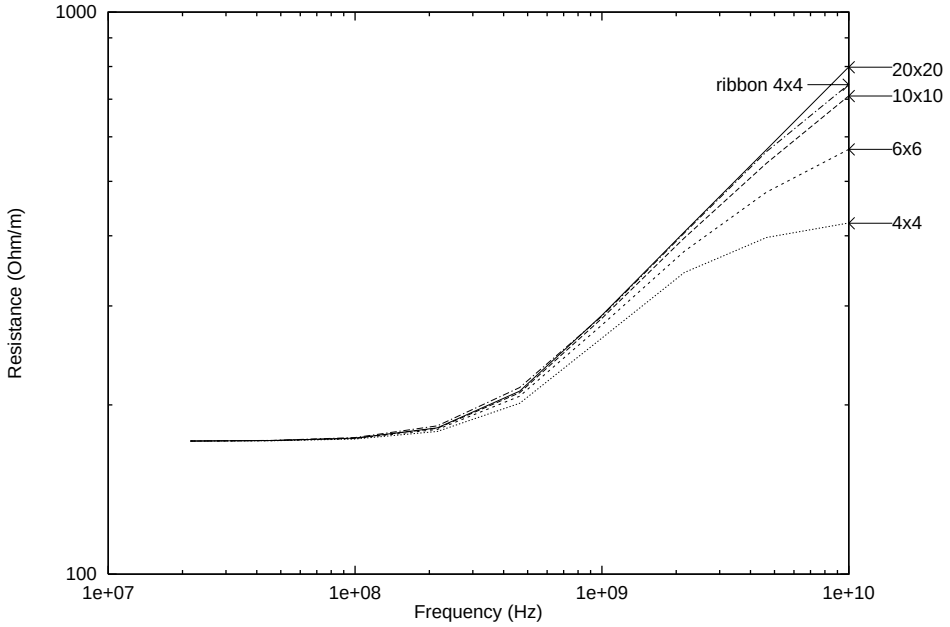

Figure 5.4: Resistance of a $10\times10\mu$m copper bar versus frequency for different mesh sizes for filament technique. The ribbon result with a mesh of 4x4 is also shown.

function.

To illustrate the advantage of using the ribbon technique, the frequency dependent resistance of a $10\mu\text{m}\times10\mu\text{m}$ square metal bar is calculated (Fig. 5.4) with different filament sizes and with the ribbon technique. In Table 5.1 the mesh sizes and corresponding CPU times for filling and solving[2] the impedance matrix are shown. In the filament technique the matrix size is $(mn)\times(mn)$ for an $m\times n$ mesh, whereas the matrix size in the ribbon technique is $2(m+n)\times 2(m+n)$ for the same mesh. Different mesh sizes are chosen to illustrate the fact that given a mesh size, the filament technique is accurate to about 10% at the frequency where the skin-depth is twice the filament size. For lower frequencies the accuracy increases. For this interconnect geometry, using adaptive meshing

[2]Gaussian elimination is used.

Technique	Mesh size	CPU (s) filling	CPU (s) solving	$f\|_{\delta/2}$ GHz	Error
Volume Filament	4×4	0.10	0.10	1.7	11%
	6×6	1.10	0.20	4.0	12%
	10×10	8.80	4.10	10.0	11%
	20×20	148.10	267.90	43.0	-
Surface Ribbon	4×4	0.10	0.10	-	5%

Table 5.1: For different mesh sizes, CPU times in seconds on a Sun Sparc 1+ Workstation for filling the matrix and solving it, the frequency where the skin-depth is equal to twice the filament size, and percentage error at that frequency compared to the 20×20 mesh size result.

with the filament technique, one can calculate the resistance of the interconnect from dc to 10GHz at three frequency points (1.7, 4.0, and 10.0 GHz) in 14.4 seconds on a Sun Sparc 1+ workstation with about 10% accuracy. With a 4×4 mesh, the ribbon technique calculation takes only 0.4 seconds to do the same frequency points with 5% accuracy.

5.3 Examples

To investigate the validity of the ribbon technique, several runs were done on various structures. The measurement results of the co-planar strips presented in Section 4.5.3 were compared to the calculation. As a second example the series resistance and inductance values obtained by the ribbon technique for a three conductor transmission line structure were compared to the filament technique results.

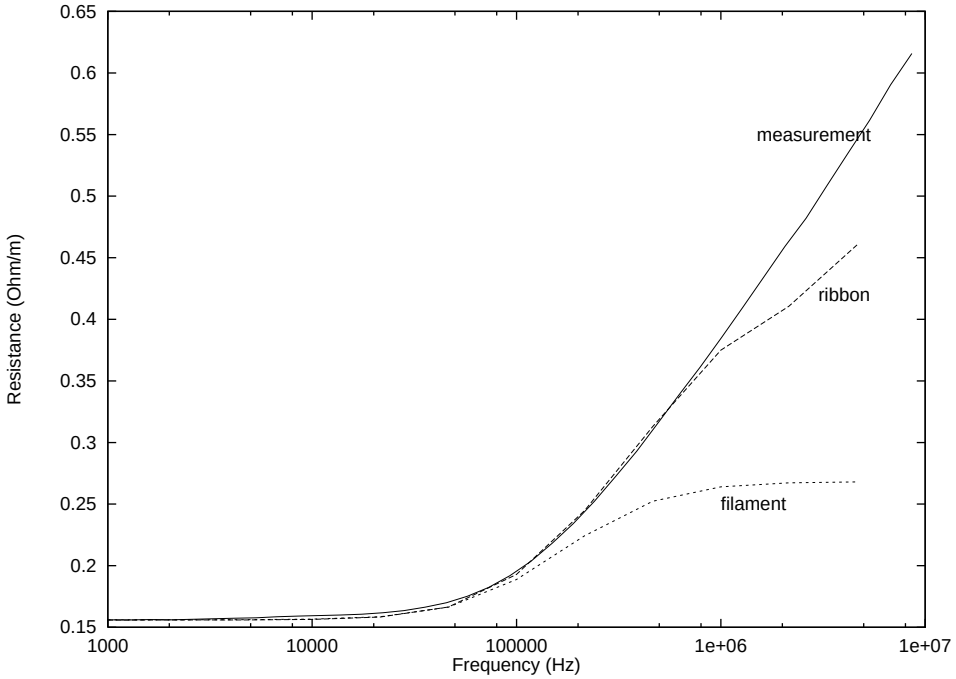

Figure 5.5: Resistance per meter versus frequency plot for a co-planar strip structure. Ribbon and filament calculations used a 5×3 mesh on each conductor.

5.3.1 Co-planar Strips

A co-planar structure was fabricated and measured as explained in Section 4.5.3. The width, thickness, and separation between the strips are 13mm, 17μm, and 1mm, respectively. The strips are made of copper ($\sigma = 5.8 \times 10^7 (\Omega\text{m})^{-1}$). In Fig. 5.5, the measurement result compared to the ribbon and filament calculations are shown for the resistive part. A 5×3 non-uniform mesh with the ratio of adjacent filament sizes (or ribbon widths) equal to 3 is used, hence the size of the filaments (width of the ribbons) is smaller near the corner. The run times for both the filament and ribbon techniques are similar (30×30 matrix size for filament and 32×32 for ribbon). But the accuracy of the ribbon technique is much better at high frequencies.

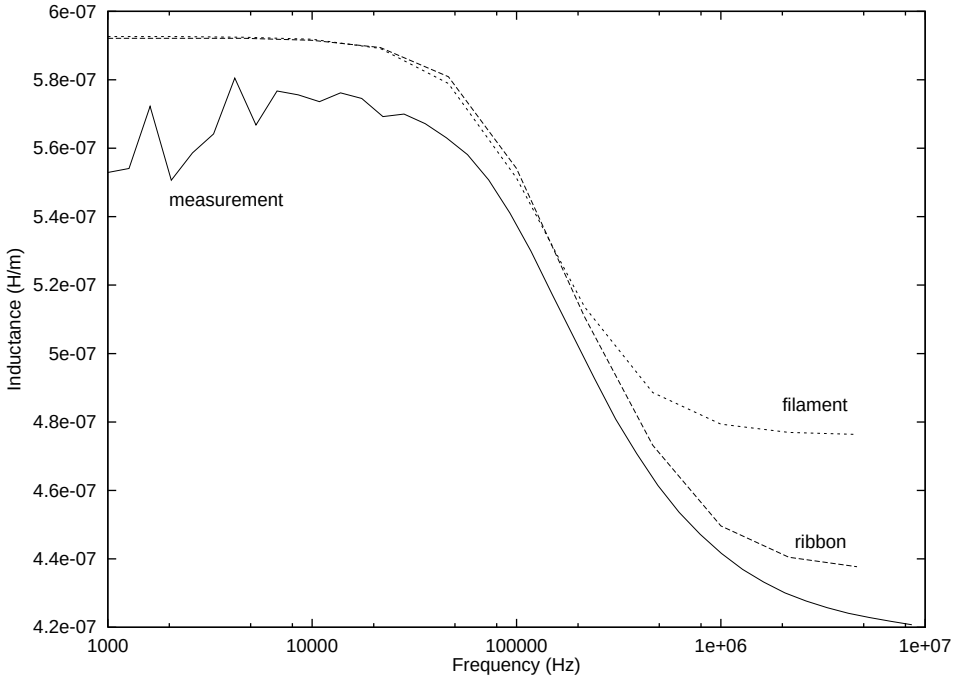

Figure 5.6: Inductance per meter versus frequency plot for the co-planar structure. Ribbon technique is more accurate at high frequencies.

At 1MHz, the ribbon technique result is within 5% of the measured value, whereas the filament technique is off by 33%. The inductance calculated by the ribbon technique is also more accurate at higher frequencies (Fig. 5.6). The dc inductances given by both techniques are in agreement and 3% higher than the measured value. At 1MHz, the ribbon technique is off by 2% compared to the filament technique's 9%. For this geometry although the run times are comparable, the ribbon technique has a superior accuracy over the filament technique.

5.3.2 Interconnect Structures

Another example to test the validity of the ribbon technique is a three conductor transmission line structure that can be an example of an interconnect structure

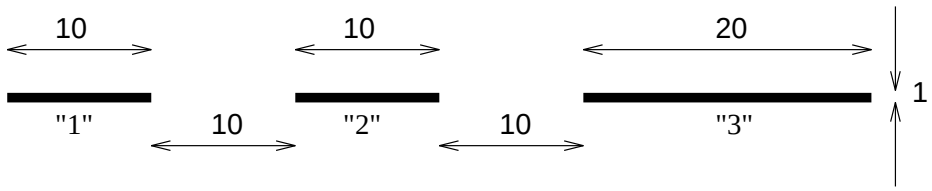

Figure 5.7: An example MCM interconnect structure, minimum feature size is 10μm. The lines are made of copper ($\sigma = 5.8 \times 10^7 (\Omega\text{m})^{-1}$). The dimensions are in micrometers (μm). Mesh sizes for the conductors are 10×3, 10×3, and 20×3, from left to right, respectively.

on a multichip module. The lines are made of 1μm thick copper with 10μm separation. The cross sectional dimensions are shown in Fig. 5.7.

The self and mutual resistance and inductance curves obtained by the filament and ribbon techniques are shown in Figs. 5.8 and 5.9, respectively. For both techniques the same size mesh was used. On a Sun Sparc 1 workstation, the calculation of the curve with the filament technique took 334 seconds of CPU time compared to the ribbon technique's 192 seconds.

For the self and mutual resistance calculation, the ribbon technique results agree with the filament technique results. It is also safe to note that the ribbon technique results are more accurate at higher frequencies than the filament technique results. A similar conclusion can be drawn for the inductance curves (Fig. 5.9),where the self and mutual inductances are within 5% of each other at low frequencies.

In this chapter a modified filament technique has been presented. Taking advantage of surface calculations, the ribbon technique is superior to the filament technique at frequencies where the skin-effect is present. With this technique, without compromising the accuracy, a faster solution is possible. Adaptive meshing can be utilized to take full advantage of both techniques: a

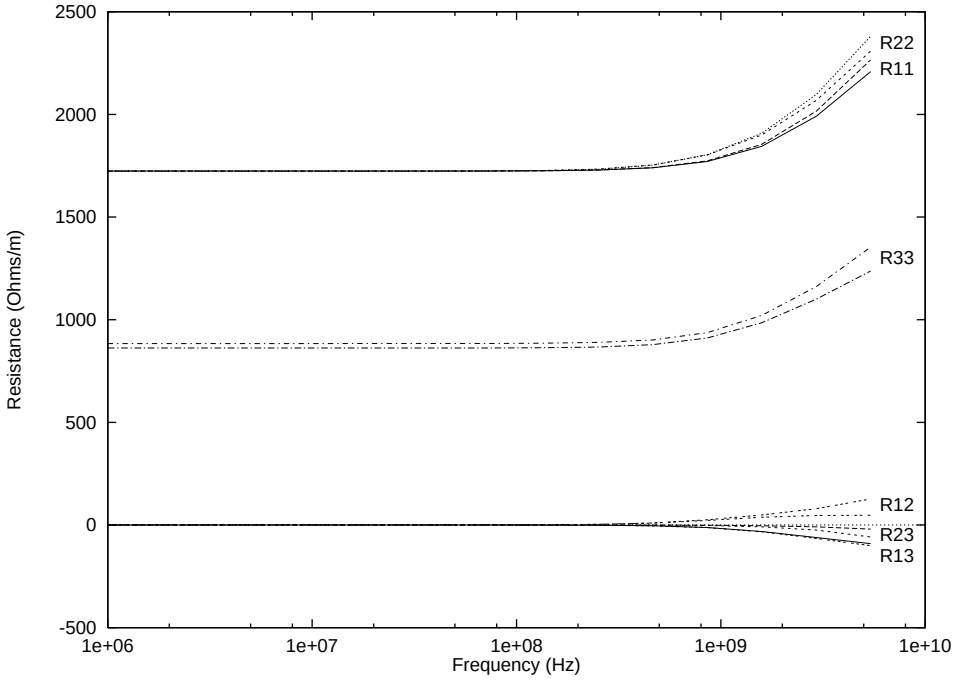

Figure 5.8: Self and mutual resistance curves of three conductor interconnect structure. Results obtained by the filament and ribbon techniques agree well. The curve with more deviation in each pair at high frequencies is calculated using the ribbon technique.

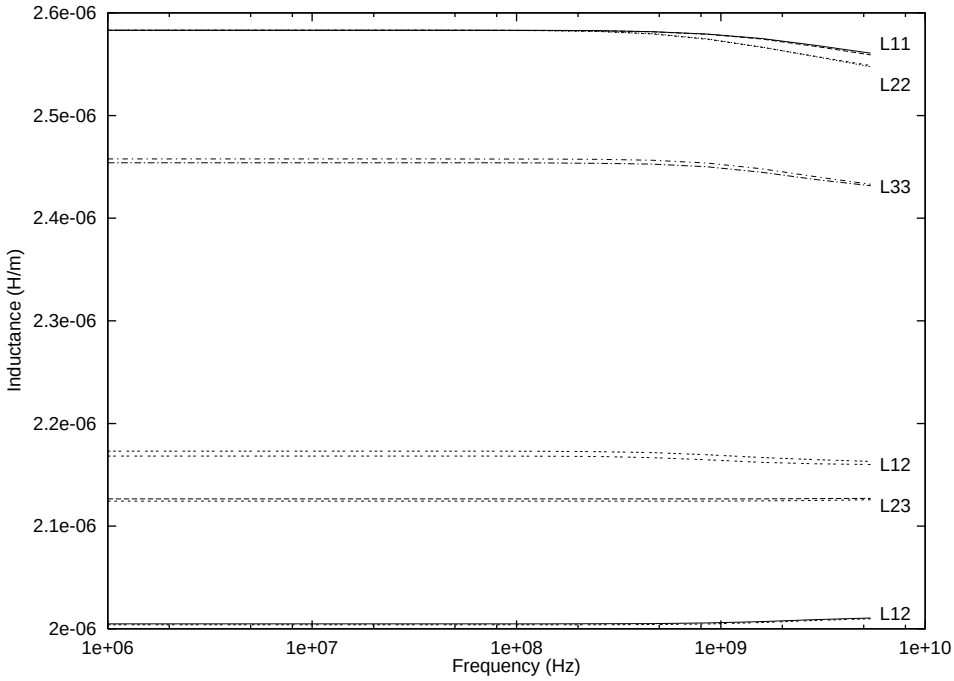

Figure 5.9: Self and mutual inductance curves of three conductor interconnect structure. Results obtained by the filament and ribbon techniques are within 5% of each other.

single filament at low frequencies and ribbons on the surface at higher frequencies. The ribbon technique is also applicable to three dimensional interconnect structures [26]. Using a modified effective internal impedance approach, the internal volume of three dimensional structures can be represented at the surface. A simpler practical application for three dimensional structures is done by incorporating the ribbon technique into FastHenry[3].

[3]More information can be obtained from the World Wide Web page at `http://weewave.mer.utexas.edu/`.